BMC Genomics

RESEARCH

Open Access

Mechanism of vitamin C alleviating the immunotoxicity of 17α-methyltestosterone in *Carassius auratus*

Tongyao Li[1], Zijun Xiong[1], Yan Liu[3], Haiyan Zhao[1], Weiya Rong[1], Yue Chen[1], Gen Chen[1], Lu Cao[1], Qing Liu[1], Jing Song[1], Weiwei Wang[1], Yu Liu[1], Xian-Zong Wang[1,4*] and Shao-Zhen Liu[1,2,4*]

Abstract

Background In recent years, the use of endocrine-disrupting chemicals (EDCs) has become increasingly common, leading to severe environmental pollution and harm to aquatic organisms. 17α-Methyltestosterone (MT) is a synthetic androgen that can cause immunotoxicity in aquaculture, affecting fish health. To address this issue, this study aimed to investigate the effect of Vitamin C (VC) on MT-induced immunotoxicity and determine the optimal VC supplementation.

Results *Carassius auratus* was exposed to 50 ng/L MT and treated with 25, 50, and 150 mg/kg VC for 7, 14, and 21 d. Morphological indicators, histological characteristics, hepatic antioxidant capacity, and immune-related gene expression were analyzed. Additionally, RNA-seq was performed on the liver tissues of the control, MT, and MT + 25 mg/kg VC groups after 21 d. Results showed that, MT treatment significantly increased liver malondialdehyde content and inhibited immune-related gene expression (*TNF-α*, *IL-8*, *INF-γ*, *IL-10*, *Caspase-9*, and *IGF-I*), causing oxidative stress and immunotoxicity, leading to hepatic steatosis. However, supplementation with 25–50 mg/kg VC effectively alleviated the MT-induced damage to the hepatic structure and immune system. RNA-seq revealed significant enrichment of differentially expressed genes in multiple signaling pathways, including the mTOR, MAPK, and Wnt pathways.

Conclusions In summary, 25–50 mg/kg VC alleviated inhibitory effect of MT on immune-related genes in *C. auratus* liver, reducing MT-induced tissue damage. VC not only alleviated inflammation, oxidative stress, and immunotoxicity induced by MT through the regulation of the mTOR, MAPK, and Wnt signaling pathways, but also indirectly enhanced cellular antioxidant defense mechanisms by regulating the NRF2 pathway. This provides a theoretical basis for VC application in aquaculture, improving fish health and increasing efficiency.

Keywords *Carassius auratus*, 17α-Methyltestosterone, Vitamin C, Immune system

*Correspondence:
Xian-Zong Wang
xianzong_wang@126.com
Shao-Zhen Liu
shmily8316@126.com

[1]College of Animal Science, Shanxi Agricultural University, Jinzhong 030801, China
[2]Shanxi Key Laboratory of Animal Genetics Resource Utilization and Breeding, Jinzhong 030801, China
[3]School of Ocean, Yantai University, Yantai 264005, China
[4]Yangjiazhuang, Jinzhong City, Taigu County, Shanxi Province, China

Background

With the rapid development of modern industries, endocrine-disrupting chemicals (EDCs) have attracted considerable attention. These substances originate from industrial wastewater, chemical factories, pesticides, and plastic pollution. Silently infiltrating ecosystems pose a threat to the health and survival of organisms. EDCs include synthetic and natural hormones, along with a spectrum of exogenous compounds that disrupt critical physiological processes [1]. These disruptions can trigger adverse effects such as reproductive dysfunction [2], developmental abnormalities [3], neurological and behavioral issues [4, 5], immune dysregulation [6], cancer, and metabolic diseases [7, 8]. Androgens play a crucial role in regulating the development and function of the immune system and the myeloid lineage, significantly affecting B and T cells in the acquired immunity of fish [9]. Testosterone exerts negative regulatory effects on the immune system by inhibiting the function of inflammatory immune cells [10]. Cytokines, key regulators of the immune system, modulate intercellular signaling and trigger immune responses [11, 12]. Studies have shown that seasonal exposure of adult *Micropterus salmoides* to 17α-ethinylestradiol can lead to immunomodulatory effects, inhibiting the mitotic activity of T cells and B cells [13], thereby impairing the normal function of the immune system. Therefore, monitoring and managing EDCs in the environment are crucial for maintaining the health of organisms.

Studies have detected 17α-Methyltestosterone (MT) concentrations as high as 250 ng/L near wastewater treatment plants, highlighting the potential for widespread environmental contamination and risks to aquatic ecosystems [14, 15]. MT is a synthetic androgen that, upon entering an animal's body, can be converted into 17-methylestradiol, a compound with estrogenic properties [16]. This conversion underpins the utility of MT in controlling sex, making it a valuable tool for enhancing aquaculture efficiency in the production of all-male fish [17, 18]. However, the use of MT negatively affects the immune system of fish [19]. Previous studies have revealed that oral administration of MT in rabbits significantly reduces the white blood cell count, indicating immune suppression and hepatotoxicity, with these deleterious effects being irreversible [20]. Similarly, injecting 17 β-estradiol into *Sparus aurata* has been shown to reduce IgM levels, resulting in immunosuppression [21].

Vitamin C (VC) is a natural antioxidant with immunomodulatory capabilities [22, 23]. VC plays a pivotal role in mitigating oxidative stress [24, 25], promoting growth, and bolstering disease resistance [26]. Furthermore, supplementing feed with 46.90-167.43 mg/kg VC can enhance the antioxidant capacity of *Lateolabrax maculatus*, thereby reducing oxidative damage [27]. Oxidative stress is characterized by an imbalance between the production of reactive oxygen species (ROS) and the cellular antioxidant defense mechanisms, which is a critical factor in the physiological processes of animals [28]. Supplementation with 60–200 mg/kg VC has been shown to markedly increase the activity of superoxide dismutase (SOD) in the plasma, thereby protecting cells from oxidative damage and reducing malondialdehyde (MDA) levels, thus safeguarding lipids from oxidation [29, 30]. Additionally, VC can mitigate oxidative damage, inflammation, and apoptosis caused by acute hypoxia in *Cyprinus carpio* by enhancing the NRF2/Kelch-like ECH-associated protein 1 (KEAP1) signaling pathway, thereby demonstrating its potent antioxidant and anti-inflammatory effects [31].

The NRF2 pathway within the immune system plays a pivotal role in the cellular antioxidant stress response, aiding the attenuation of pro-inflammatory activity in immune cells during infections [32]. Research indicates that NRF2 exhibits prominent expression within the liver, where it effectively counters elevated levels of ROS, thereby maintaining liver homeostasis, facilitating chemical detoxification and drug metabolism, and protecting cells from oxidative stress-induced damage [33]. Mice experiments corroborate these findings, as NRF2 knockout models exhibit heightened inflammation, diminished steroidogenesis, compromised antioxidant capacity, and elevated expression of ROS markers [34]. Furthermore, research indicates that VC acts as an activator of the NRF2 factor and the comprehensive KEAP1/NRF2/antioxidant response elements (ARE) pathway. Insufficient VC levels can impair NRF2 function, leading to inflammation and apoptosis [35].

In this study, we selected *Carassius auratus* as the research subject. *Carassius auratus* was subjected to varying concentrations of MT and VC for 7, 14, and 21 d. We evaluated the expression of immune-related genes and antioxidant enzyme activity. Based on preliminary findings, we conducted RNA-seq analysis on liver tissues in the control, 50 ng/L MT, and 50 ng/L MT + 25 mg/kg VC groups after 21 d of exposure to investigate how VC alleviates MT-induced immunotoxicity. This study provides an important reference for the healthy aquaculture of *C. auratus* and offers a theoretical basis for mitigating the toxicity associated with other EDCs.

Methods

Experimental animals

We selected 4-month-old females of *C. auratus*, bred from the same batch at the Aquaculture Laboratory of Shanxi Agricultural University. The fish were acclimatized for 7 d in aerated tap water with a stocking density of 1 g fish/L. They were fed at a rate of 3% of the total fish weight in each experimental group. Water quality

was maintained at a temperature of 21.5±0.3 ℃, a pH of 7.45±0.2, and dissolved oxygen levels≥7 mg/L under a light/dark cycle of 14 h: 10 h. A total of 450 healthy fish (10.61±2.94 g) were randomly selected and divided into five groups (21 fish per group, with three replicates each): control group, 50 ng/L MT group, 50 ng/L MT+25 mg/kg VC group, 50 ng/L MT+50 mg/kg VC group, and 50 ng/L MT+150 mg/kg VC group.

Experimental feeds and design

The experiment used specialized feed for *C. auratus* (153 floating feed, produced by Tongwei Co., Ltd.) as the basal diet. The composition of this feed included moisture content≤12%, crude protein≥32%, crude ether extract≥5%, and crude fiber≤8.5%. Based on the experimental groups, VC (Sinopharm Chemical Reagent Co., Ltd.) was added at concentrations of 0, 25, 50, and 150 mg/kg. The feed preparation method followed the procedure described by Mi et al. [36]. The VC content was determined using the direct iodometric method [37]. During the experiment, 50% of the water was changed daily, with food residues and excrement removed during water changes. A corresponding amount of MT reagent was added during the water change to maintain a constant MT concentration in the water. Sampling was conducted at 7, 14, and 21 d. Detailed results are presented in Table 1.

Sample collection and biological parameter determination

Following the exposure experiment, 21 fish from each group were selected and anesthetized using MS-222 (1:10,000). The body length, body weight, and liver weight of each fish were measured to calculate the hepatic steatosis index (HSI). Liver tissues from 6 randomly selected fish per group were collected for histological analyses. These tissues were fixed in Bouin's fixative solution (Phygene, Fuzhou, China) for 24–48 h to facilitate paraffin embedding and sectioning. The remaining 15 fish were rapidly frozen in liquid nitrogen and stored at -80 ℃ for subsequent analyses. Among these, 6 liver samples were designated for RT-qPCR, 6 for enzyme activity assays, and 3 for RNA-seq.

Paraffin section preparation and observation

Liver tissue samples were extracted from Bouin's fixative solution, rinsed with piped water for 24 h, and subjected to dehydration, embedding, and staining procedures. The paraffin sectioning method was adapted from our previous research [38].

RT-qPCR detection of immune-related gene mRNA expression in the liver

To assess the immune toxicity induced by MT and the mitigating effects of VC, we selected a series of important genes related to immune response and oxidative stress. These genes include tumor necrosis factor-alpha (*TNF-α*), interleukin-8/10 (*IL-8* and *IL-10*), interferon-gamma (*IFN-γ*), transforming growth factor-beta 1 (*TGF-β1*), chemokine (C-X-C motif) (*CXC*), cysteinyl aspartate specific proteinase 9 (*Caspase-9*), and insulin-like growth factor I (*IGF-I*), with gene sequences obtained from the National Center for Biotechnology Information (NCBI) (bioproject: PRJNA481500) for *C. auratus* [39]. The primers for these genes were designed using Primer Premier 5.0 software, with *β-actin* as the housekeeping gene. The primers were synthesized by Sangon Biotech (Shanghai, China), and the specific sequences used in RT-qPCR are listed in Table 2.

Total RNA was isolated from the liver tissue using the TRIzol method. RNA integrity was evaluated using 1% agarose gel electrophoresis, and the purity and concentration were determined using a NanoDrop spectrophotometer (Thermo Fisher Scientific, USA), ensuring an $OD_{260/280}$ ratio within the normal range of 1.8 to 2.1. Qualified RNA samples (5 μL) were used for reverse transcription to synthesize first-strand cDNA, employing the PrimeScript™ RT Reagent Kit with gDNA Eraser (Perfect Real Time, TaKaRa). The resulting cDNA products were stored at -80 °C for subsequent RT-qPCR detection.

RT-qPCR was conducted using the TB Green Premix Ex Taq™ II (Tli RNaseH Plus) (TaKaRa) system. Each tissue sample underwent triplicate runs to ensure robustness and accuracy. Utilizing the reverse-transcribed cDNA as a template, we assessed changes in the expression levels of immune-related genes in liver tissues after MT and VC treatments.

Preparation of liver tissue homogenate and determination of antioxidant enzymes

Liver tissue homogenate preparation and analysis

Liver tissue samples were retrieved from the −80 ℃ freezer and weighed, with 0.1 g of tissue blocks subsequently mixed with a pre-cooled 0.86% NaCl solution at

Table 1 Determination of VC content in feeds. Number of sample replicates $n=3$

Method	Nominal VC content (mg/kg)	Actual VC content (mg/kg)				Standard deviation
		N1	N2	N3	Average	
Iodometric method	0	8.8065	5.2839	8.8065	7.6323	2.00338
	25	26.4195	21.1356	35.2260	27.5937	7.11821
	50	52.8390	49.3164	61.6455	54.6003	6.35046
	150	176.1300	140.9040	158.5170	158.5170	17.61300

Table 2 Sequences of primer pairs used in the RT-qPCR

Categorization	Genes	Primer sequence (5′-3′)	TM (℃)	GenBank
Housekeeping	*β-actin*	F: GCAGATGTGGATTAGCAAGCAG	57	XM_026211398.1
		R: TTGAGTCGGCGTGAAGTGG	57	
Immune	*TNF-α*	F: GCCATCCATTTAACAGGTGCAT	57	XM_026256406.1
		R: GCTAATTTCAAGCCGCCTGAA	57	
	IL-8	F: TAGATCCACGCTGTCGCTG	57	XM_026266346.1
		R: AGGGTGCTTTAGGGTCCAG	57	
	IFN-γ	F: GCACTTTTGCCTGGGAAGTAG	57	AY452069.1
		R: CAGTAGGATATTCACTCGCATGG	57	
	TGF-β1	F: AATCACGCTTTATTTCCGAC	57	XM_026234919.1
		R: TGTATCCACTTCCAGCCCAG	57	
	IL-10	F: GCAACAGCACATCAACAGTCCT	57	XM_026275831
		R: CTGGCGAACTCAAAGGGATT	57	
Chemotactic	*CXC*	F: CGTTACGATGACTGATCCGAATA	57	XM_026271209
		R: GCCTTTTTTTGTTGGAGGTGAT	57	
Apoptosis	*Caspase-9*	F: CAGGCGTAATCTAGTCAAGGCA	57	XM_026241892.1
		R: GACAGAAGGAGACAGACGAGCAC	57	
Growth	*IGF-I*	F: CAAATCCGTCTCCTGTTCGCTA	57	XM_026232874
		R: CCCTGGAAGAAATGACCGCTA	57	

a ratio of 1: 9. The mixture was homogenized to obtain a 10% tissue homogenate using an automated sample rapid grinding instrument (Jingxin, Shanghai, China). Following homogenization, the samples were centrifuged at 3,000 rpm for 10–15 min to obtain the supernatant for analysis. The 10% tissue homogenate was further diluted to 1%, and the protein concentration was determined using a BCA Protein Assay Kit (Boster Bio, Wuhan, China). OD values were measured, and protein concentrations were calculated using a standard curve (with X representing protein concentration in μg/ml and Y representing the final OD_{562nm} value). The correlation coefficient of the standard curve is $R^2=0.9988$.

Measurement of antioxidant enzymes in C. auratus liver

The activities of MDA, SOD, and glutathione peroxidase (GSH-PX) were measured using TBA, WAT-1, and colorimetric assays, respectively. All assay kits were purchased from Nanjing Jiancheng Bioengineering Institute, and the procedures were performed according to the manufacturer's instructions.

RNA-seq analysis and validation

RNA extraction and cDNA library construction

In this study, liver tissues from the control group (CT), 50 ng/L MT group (MT), and MT+25 mg/kg VC group (MT+L) at 21 d were selected for RNA-seq analysis. RNA extraction was performed using the TRIzol method, and RNA quality was evaluated using a NanoDrop 2,000. Eukaryotic mRNA with poly-A tails was enriched using magnetic beads coupled to oligo(dT). Subsequently, cDNA synthesis and library construction were carried out. After PCR amplification and quantification, RNA integrity was precisely evaluated using an Agilent 2,100 system. The RNA-seq library construction and sequencing were conducted by Gene denovo Biotechnology Co., Ltd. (Guangzhou, China), resulting in nine sequencing libraries.

Screening and annotation of differentially expressed genes (DEGs)

Initially, the raw reads underwent quality control processing using fastp, which removed adapter sequences, reads with an N ratio > 10%, reads composed entirely of A bases, and low-quality reads. This resulted in the generation of high-quality clean reads. Subsequently, HISAT2 (http://daehwankimlab.github.io/hisat2) was used to align these reads to the reference genome (NCBI_GCF_003368295.1) and calculate their genomic distribution. Transcripts were reconstructed using the Stringtie, and gene expression levels for each sample were quantified using RSEM.

To ensure the reliability of subsequent analyses, sequencing depth and gene/transcript length were normalized to obtain fragments per kilobase million (FPKM) values. Based on the expression levels of each sample, the Pearson correlation coefficients between samples were calculated to assess sample reproducibility. The correlation heatmap was created using the R software. DEGs were identified using DESeq2 with criteria of fold change (FC) ≥ 1.8 and $P<0.05$, and enrichment analysis was performed on these DEGs.

Validation of DGEs

To validate the RNA-seq results, eight DEGs were selected for verification: proteasome non-ATPase

regulatory subunit 6 (*PSMD6*), C-C motif chemokine 2 (*CCL2*), C-X-C motif chemokine 2 (*CXCL*), nuclear factor erythroid 2-related factor 2 (*NFE2L2*), ferritin (*FTH*), *KEAP1*, mannosyl-oligosaccharide 1 (*MAN1A1*), and bone morphogenetic protein receptor type-1B (*BMPR1B*). Primers for these DEGs were designed using the Primer Premier software for RT-qPCR validation. The primers were synthesized by Sangon Biotech (Shanghai, China). The primer sequences are listed in Table 3.

Enrichment analysis of gene ontology (GO) and Kyoto encyclopedia of genes and genomes (KEGG)

Enrichment analysis of GO terms and KEGG pathways were performed on the identified DEGs to identify key genes associated with specific biological processes and pathways. GO is an internationally standardized classification system for gene functions, including molecular functions (MF), biological processes (BP), and cellular components (CC). KEGG provides insights into the biological pathways involving these DEGs, ranging from metabolic pathways to signaling pathways. These analyses contributed to a comprehensive understanding of the biological functions and regulatory mechanisms of DEGs.

Data analysis

In this experiment, data analysis for RT-qPCR was conducted using the $2^{-\triangle\triangle Cq}$ method. All data were expressed as mean ± SD. Statistical analysis was carried out with IBM SPSS Statistics 24.0, employing one-way analysis of variance (ANOVA) and the least significant difference (LSD) method to evaluate the significance of differences. Statistical significance was defined as $P<0.05$ and is denoted by different lowercase letters. Graphs and charts were generated using the GraphPad Prism 8.3.0 software.

Results

Effects of MT and various doses of VC on biological indices in *C. auratus*

Carassius auratus were exposed to 50 ng/L MT and different doses of VC (25, 50, and 150 mg/kg) for 7, 14, and 21 d. With the increase in exposure duration, the morphological indicators of the fish displayed varying degrees of growth. For ease of reference, the groups are abbreviated as follows: control group (CT), 50 ng/L MT group (MT), MT + 25 mg/kg VC group (MT + L), MT + 50 mg/kg VC group (MT + M), and MT + 150 mg/kg VC group (MT + H), respectively.

After 7 d of exposure, the liver weight and HSI of the MT + M group significantly increased. When the exposure time was extended to 14 d, the body lengths of the MT group and MT + H groups showed a significant increase. Additionally, liver weight and HSI of the MT group significantly increased (Table 4).

Effects of MT and varied VC dosages on the histology of liver tissues in *C. auratus*

Histological examination of the paraffin sections revealed significant changes in liver tissue morphology over time. At 7 d, the liver cells in the CT group exhibited regular morphology with clear boundaries and a uniform

Table 3 DEGs primer sequence information

Genes	Primer sequence (5′-3′)	TM (℃)	GenBank
PSMD6	F: GCTGAGAAGAACCAGGGAGAG	57	LOC113092087
	R: AGCGATGACCAAGAGCAACG	57	
CCL2	F: TGCTGTTGCTGTGTGTCTTGG	57	LOC113045414
	R: GACCTGTCTGTTCTTCACCGTAG	57	
CXCL	F: ATGCTCTCTTTCGTTCTGCTGG	57	LOC113049114
	R: AACTGTTTGGTTGTCCTTTTTGG	57	
FABP2	F: GAAAGTGGACCGCAATGAAAA	57	LOC113084692
	R: CAAAGTTGACGCCGAGAGTAAAG	57	
FTH	F: ATGTGGGGCAATGGACTGAT	57	LOC113047393
	R: TGGAAAGGTTGGTGATGTGGT	57	
POLR2E	F: CAGAGGAGATGAAAGTGGGCA	57	LOC113112300
	R: CAAAGACTGTTTAGCAGAGGGTGT	57	
BMPR1B	F: GTGAAGCAGATCGGGAAGGG	57	LOC113069268
	R: GCGTGGTGGATTTGAGGTAGT	57	
MAN1A1	F: TTTTCTTCCGCTCGTCCTCG	57	LOC113079829
	R: ATCCTTTCCCCTGTCCGTTTA	57	
NFE2L2	F: CACAGGACCCAAACTACAGCC	57	XM_026272638.1
	R: CATCAGGGACGAGAGGACCAC	57	
KEAP1	F: CCTCTACACATCACAACAGCGT	57	XM_026290136
	R: CCAACCACATACAGACTTCCCC	57	

Table 4 Changes in morphological indices and HSI of *C. Auratus*. Multiple treatment groups were established for this experiment. All data are presented as mean ± SD. Values without letters or with the same letters in the same column indicate no significant difference ($P < 0.05$). Lowercase letters indicate statistically significant differences

Exposure time	Groups	Body length (cm)	Body weight (g)	Liver weight (g)	HSI (%)
7 d	CT	7.35 ± 0.62^{ab}	10.6091 ± 2.9355	0.520 ± 0.166^{bc}	0.049 ± 0.009^{bc}
	MT	7.36 ± 0.48 ^{ab}	11.6174 ± 2.2283	0.621 ± 0.235^{ab}	0.052 ± 0.017^{ab}
	MT + L	7.15 ± 0.83 ^{b}	10.1202 ± 4.4232	0.467 ± 0.201^{c}	0.046 ± 0.015^{bc}
	MT + M	7.23 ± 0.42 ^{ab}	11.2075 ± 2.1715	**0.710 ± 0.248^{a}**	**0.062 ± 0.017^{a}**
	MT + H	7.58 ± 0.81 ^{a}	11.9875 ± 3.8844	0.502 ± 0.286^{bc}	0.041 ± 0.023^{c}
14 d	CT	7.20 ± 0.32^{b}	10.6775 ± 2.0173	0.498 ± 0.168^{b}	0.047 ± 0.012^{bc}
	MT	**7.82 ± 0.79^{a}**	12.5721 ± 3.1796	**0.675 ± 0.171^{a}**	**0.055 ± 0.012^{a}**
	MT + L	7.38 ± 0.96^{ab}	11.6200 ± 2.8235	0.607 ± 0.150^{ab}	0.053 ± 0.011^{ab}
	MT + M	7.20 ± 0.71^{b}	10.9940 ± 4.7008	0.602 ± 0.264^{ab}	0.052 ± 0.013^{abc}
	MT + H	**7.80 ± 0.75^{a}**	12.1545 ± 3.5755	0.544 ± 0.143^{b}	0.046 ± 0.008^{c}
21 d	CT	7.83 ± 0.91	12.1659 ± 4.0102	0.658 ± 0.301	0.054 ± 0.019 ^{ab}
	MT	8.06 ± 0.93	13.3559 ± 4.1637	0.666 ± 0.268	0.050 ± 0.010 ^{ab}
	MT + L	7.71 ± 0.62	11.6809 ± 2.7873	0.621 ± 0.287	0.052 ± 0.015 ^{ab}
	MT + M	7.83 ± 0.63	12.6908 ± 2.9007	0.737 ± 0.180	0.058 ± 0.008 ^{a}
	MT + H	7.80 ± 0.87	12.3682 ± 3.8897	0.601 ± 0.271	0.048 ± 0.011 ^{b}

arrangement. In contrast, the MT group exhibited signs of karyolysis, pyknosis, and fatty degeneration in the liver. The MT + L group displayed initial signs of liver cell normalization, although nuclear pyknosis was evident. The liver tissue structure and cell morphology in the MT + M group appeared largely normal, with a notable decrease in fatty degeneration. Conversely, the MT + H group exhibited a disorganized liver cell structure, irregular cell morphology, and unclear boundaries, accompanied by signs of karyolysis. By 14 d, the MT group displayed severe fatty degeneration of the liver, with nuclear pyknosis and karyolysis. The MT + L group showed reduced fat degeneration, whereas the MT + M group had mostly normal cell structures, albeit with some instances of nuclear pyknosis. The MT + H group experienced significant structural damage to the liver cells, severe fatty degeneration, and pronounced karyolysis. At 21 d, the MT group presented with severe liver fatty degeneration and marked nuclear pyknosis. In contrast, liver cell morphology in the MT + L and MT + M groups gradually improved, with a reduction in nuclear pyknosis and karyolysis. However, the MT + H group continued to show significant liver cell morphological damage and nuclear pyknosis (Fig. 1).

Effects of MT and varied VC dosages on the expression of immune-related genes in *C. auratus*

Significant alterations in the expression of immune-related genes were observed in liver tissues. At 7 d, compared to the CT group, the MT group, MT + M group, and MT + H group all exhibited significantly decreased *TNF-α* mRNA expression, along with a significant reduction in *IL-8* mRNA expression across all treatment groups. Upon extending the exposure to 14 d, the *TNF-α* and *IL-8* mRNA expression levels significantly increased in the MT + L and MT + M groups, whereas *INF-γ* mRNA expression significantly decreased in all treatment groups. At 21 d, *IL-8* mRNA expression significantly decreased in all treatment groups, whereas *INF-γ* mRNA expression significantly increased in the MT + L group (Fig. 2A-C). Regarding anti-inflammatory cytokines, on 7 d, *IL-10* mRNA expression was significantly reduced in the MT group compared to the CT group, while *TGF-β1* mRNA expression significantly decreased in the MT + L, MT + M, and MT + H groups. By 14 d, *IL-10* mRNA expression significantly decreased in the MT + H group, whereas *TGF-β1* mRNA expression significantly increased in the MT, MT + L, and MT + H groups. At 21 d, *IL-10* mRNA expression significantly decreased in the MT + L and MT + M groups, whereas *TGF-β1* mRNA expression significantly increased in the MT + M group (Fig. 2D-E). In terms of chemotactic factors, at 7 d, *CXC* mRNA expression was significantly higher in the MT + H group than in the CT group. By 14 d, *CXC* mRNA expression was significantly increased in the MT + L and MT + M groups. However, at 21 d, *CXC* mRNA expression was significantly increased in the MT + L group (Fig. 2F). Regarding apoptosis-related genes, at 7 d, *Caspase-9* mRNA expression significantly decreased in the MT and MT + H groups compared to the CT group. By 14 d, *Caspase-9* mRNA expression significantly increased in the MT + L group, but significantly decreased in the MT + H group (Fig. 2G). Regarding growth factors, at 7 d, all treatment groups exhibited a significant decrease in *IGF-I* mRNA expression compared to the CT group. However, by 14 d, *IGF-I* mRNA expression significantly increased in the MT + L, MT + M, and MT + H groups. By

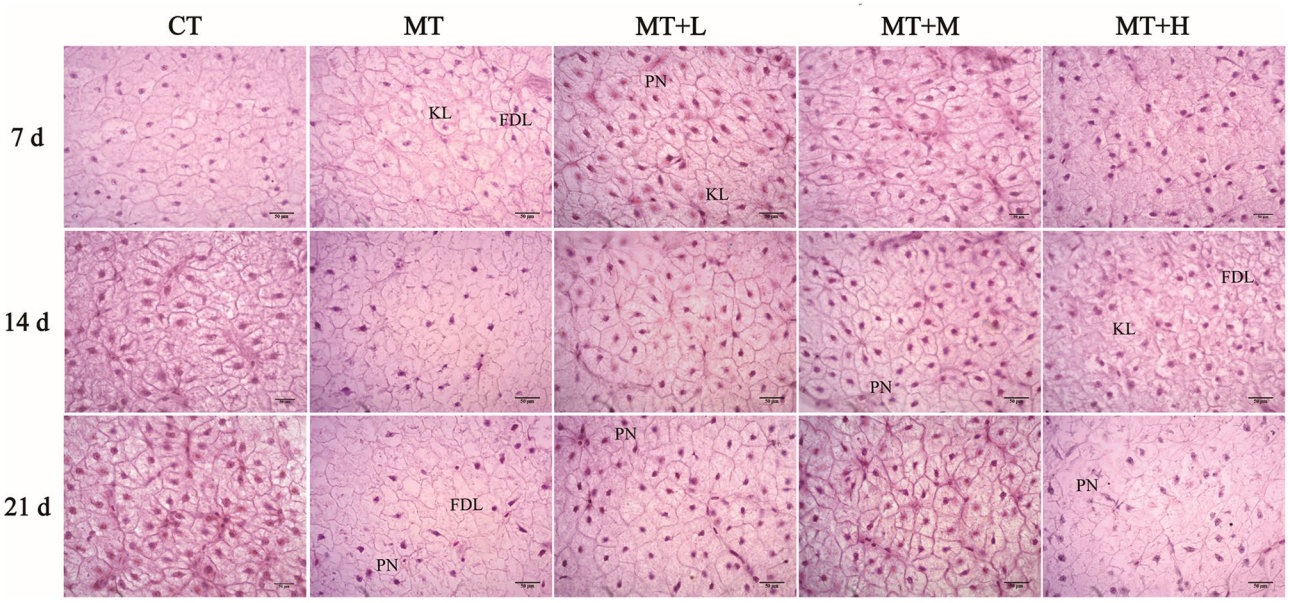

Fig. 1 Histological changes in the liver tissue of *C. auratus* exposed to MT and varied doses of VC (H & E staining, scale bar = 50 μm). Column CT represents the control group; Column MT represents the 50 ng/L MT group; Column MT + L represents the MT + 25 mg/kg VC group; Column MT + M represents the MT + 50 mg/kg VC group; and Column MT + H represents the MT + 150 mg/kg VC group. KL stands for karyolysis, PN stands for nuclear pyknosis, and FDL stands for fatty degeneration of the liver

21 d, *IGF-I* mRNA expression significantly increased in the MT + L and MT + H groups (Fig. 2H).

Effects of MT and varied VC dosages on the antioxidant capacity of *C. auratus*

At 14 d, SOD activity was significantly higher in the MT + H group than in the CT group, followed by a notable increase in SOD activity in both the MT and MT + H groups at 21 d (Fig. 3A). At 7 d, compared to the CT group, MDA content significantly increased in the MT group, whereas it markedly decreased in the MT + M and MT + H groups. After 14 d, the MDA content significantly decreased in the MT + L group but significantly increased in the MT + H group. Extending the exposure time to 21 d resulted in a significant decrease in MDA content in all treatment groups (Fig. 3B). At 7 d, compared to the CT group, GSH-PX activity significantly increased in the MT + L, MT + M, and MT + H groups. By 14 and 21 d, GSH-PX activity significantly increased in all treatment groups (Fig. 3C).

RNA-seq analysis of MT and VC effects on *C. auratus* liver

Quality control analysis of sequencing data

Using the Illumina HiSeq platform, we obtained 377,840,856 raw reads from the nine liver samples. After filtering out low-quality sequences, 376,703,854 clean reads were acquired (Table 5), with an average GC content of 47.80%. The de novo assembly of these clean reads resulted in the identification of 55,973 transcript sequences. To assess the correlation between samples from the CT, MT, and MT + L groups, we performed a Pearson correlation coefficient analysis and generated a heatmap to display the correlations. The results indicated correlation coefficients exceeding 0.86, signifying a high degree of similarity among samples (Fig. 4A), which attests to the high accuracy of the RNA-seq data.

Using DESeq2 R software, we conducted a significance analysis on 20,215 identified genes, setting thresholds of $P < 0.05$ and FC ≥ 1.8. Our analysis revealed that 1,360 genes were significantly altered in the MT group, comprising 595 upregulated and 765 downregulated genes. In the MT + L group, 3,813 genes exhibited significant changes, including 3,123 upregulated and 690 downregulated genes (Fig. 4B). A Venn diagram was used to discern common and unique genes among groups. The results identified 14,393 common genes, whereas the CT, MT, and MT + L groups contained 618,497, and 2,522 unique genes, respectively (Fig. 4C). Finally, we performed a heatmap analysis targeting DEGs in the hepatocellular carcinoma pathway to illustrate the expression patterns of these genes under various treatment conditions and the clustering patterns among the samples (Fig. 4D).

GO and KEGG enrichment analysis

For GO and KEGG enrichment analyses, we mapped the transcripts of the DEGs in the hepatocellular carcinoma pathway to the GO database. This enabled us to assess the potential functions of the significant DEGs at the transcriptional level following MT and VC treatments, both individually and in combination. The identified and

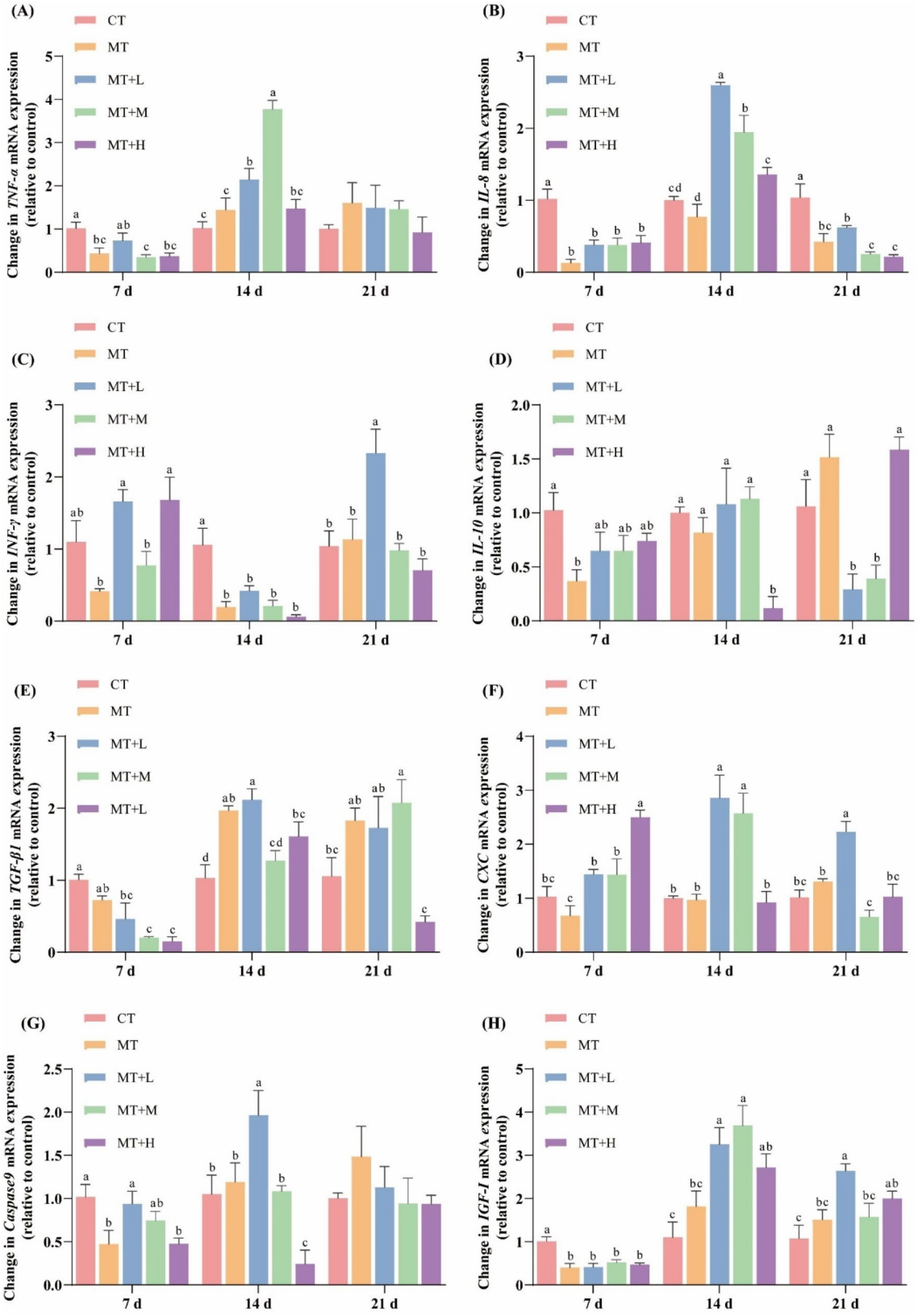

Fig. 2 Effects of MT and various doses of VC on the expression of *TNF-α* (**A**), *IL-8* (**B**), *INF-γ* (**C**), *IL-10* (**D**), *TGF-β1* (**E**), *CXC* (**F**), *Caspase-9* (**G**), and *IGF-I* (**H**) in the liver of *C. auratus*

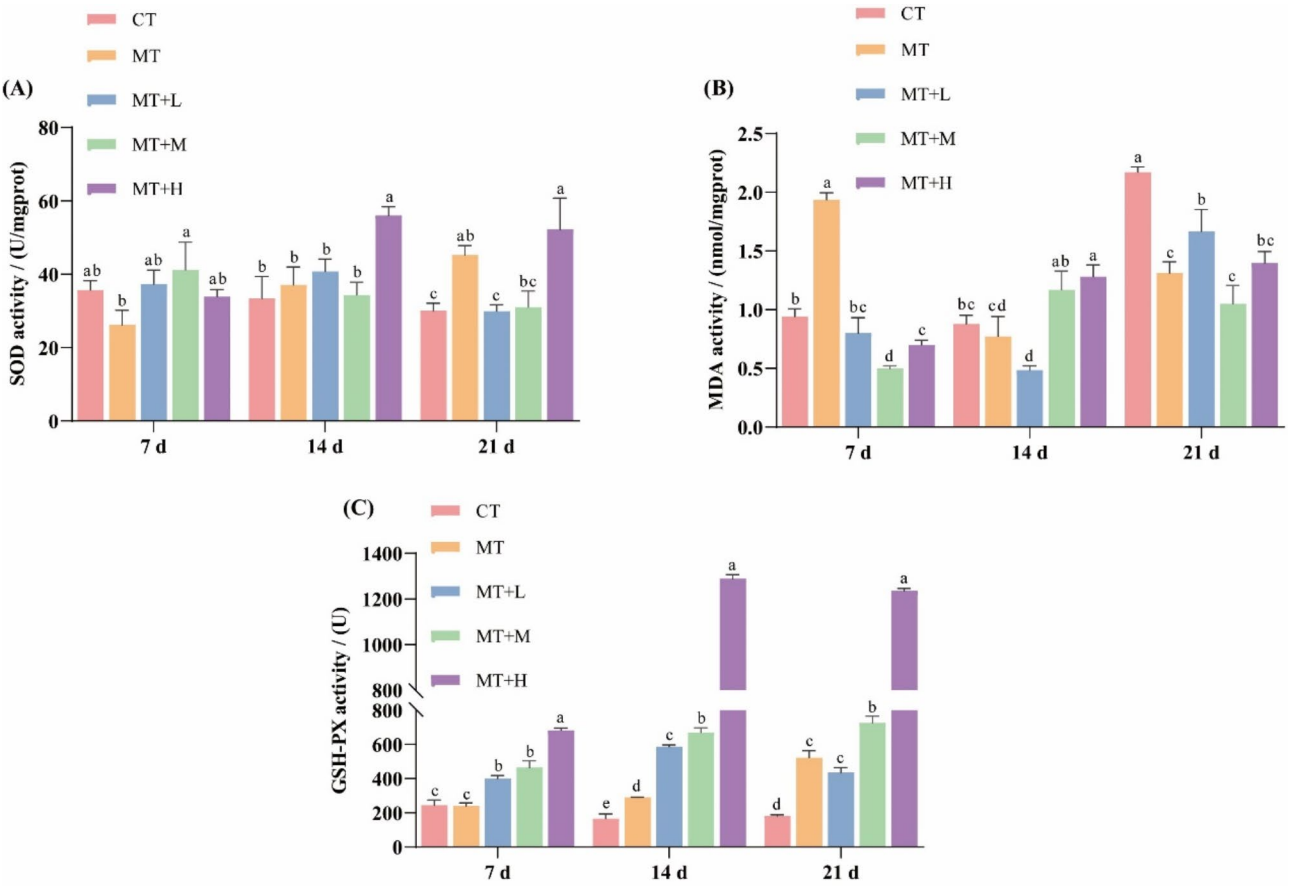

Fig. 3 Effects of MT and varied VC dosages on SOD, MDA, and GSH-PX in the liver of *C. auratus*

Table 5 Summary of the transcriptome of *C. Auratus*. Q30: percentage of nucleotides with a quality value > 30 in reads (the error rate is less than 0.1%); the higher the value, the better the sequencing quality

Sample	Raw reads	Raw data (bp)	Clean reads	Clean data (bp)	Clean reads rate (%)	Clean q30 bases rate (%)
Control-1	45,798,676	6,869,801,400	45,679,128	6,803,813,721	99.74	93.19
Control-2	41,286,262	6,192,939,300	41,146,982	6,118,859,803	99.66	93.61
Control-3	40,918,104	6,137,715,600	40,781,446	6,061,170,131	99.67	93.03
MT-1	42,402,342	6,360,351,300	42,282,380	6,292,071,838	99.72	93.33
MT-2	37,744,756	5,661,713,400	37,627,180	5,608,363,353	99.69	93.11
MT-3	43,856,836	6,578,525,400	43,720,126	6,500,707,401	99.69	93.19
MT + L-1	39,290,826	5,893,623,900	39,173,172	5,834,589,326	99.70	93.23
MT + L-2	43,793,304	6,568,995,600	43,684,938	6,515,049,724	99.75	93.39
MT + L-3	42,749,750	6,412,462,500	42,608,502	6,351,720,750	99.67	93.12

predicted transcripts were categorized into three groups: those involved in BP, cellular CC, and MF. Within the *C. auratus* transcriptome, GO functional enrichment analysis revealed that 169 genes were implicated in BP, 45 were associated with CC, and 29 were linked to MF. Specifically, BP encompasses cellular processes, single-organism processes, and the regulation of biological processes. CC include binding, catalytic activity, nucleic acid-binding transcription factor activity, and molecular function regulators. The MF involves cells, cell parts, organelles, and extracellular regions (Fig. 5A). KEGG analysis showed that the DEGs were significantly enriched in various cancer-related pathways. Furthermore, they were notably enriched in the mTOR, MAPK, and Wnt signaling pathways (Fig. 5B).

Enrichment trend analysis

The findings demonstrated that 45 target DEGs were categorized into 8 distinct gene expression patterns (Fig. 6A). Among these, 10 target DEGs were found in profiles 0 and 7, and 12 target DEGs were found in profile 4. Notably, in profile 4, genes *FZD7-A*, *WNT8A*, *GSTO1*,

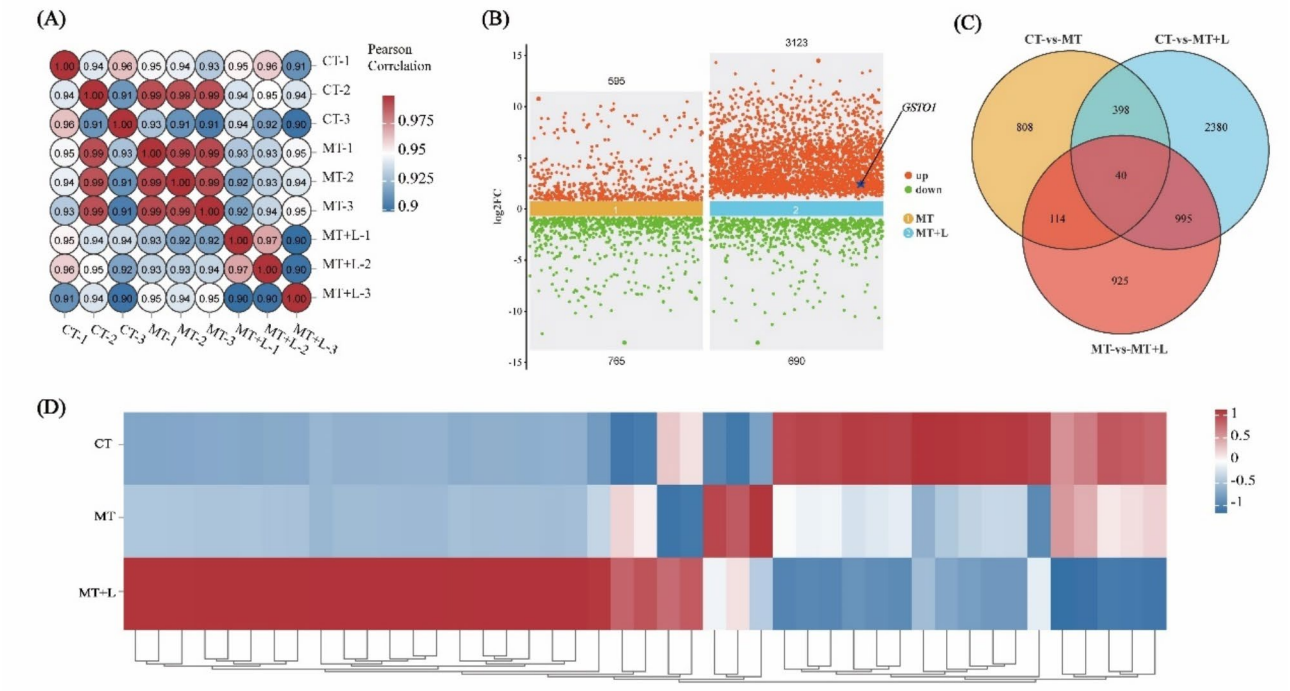

Fig. 4 Transcriptome differential gene expression. (**A**) Pearson's correlation coefficients were calculated to determine sample correlations and are displayed in a heatmap. (**B**) A multi-group differential scatter plot was created, with the y-axis representing log2FC and the x-axis representing the names of the comparison groups. (**C**) A Venn diagram was drawn to analyze the intersections of different sets after filtering for gene abundance. (**D**) A heatmap of target genes was plotted, with gene expression levels standardized using z-scores; the y-axis represents sample names, and the x-axis represents gene names

GADD45A, *MYCN*, and *E2F2* exhibited downward trends in the MT group. Conversely, these genes were upregulated in the MT+L group (Fig. 6B).

Validation of DEGs

To corroborate the RNA-seq findings, we selected eight DEGs for RT-qPCR analysis. As depicted in Fig. 7, despite minor discrepancies between the RT-qPCR results and RNA-seq data, the overall trends were consistent. This consistency underscores the reliability of the RNA-seq data.

Discussion

Effects of VC on mitigating MT-induced histological changes in the liver of *C. auratus*

Studies have demonstrated that androgens, such as steroid hormones, primarily influence the reproductive system development. However, they are also associated with hepatotoxicity and adverse effects on the immune system [40]. Conversely, VC prevents DNA mutations, inflammation, and apoptosis. In clinical trials, high-dose intravenous VC has been widely used to treat various cancers, including glioblastoma, ovarian cancer, prostate cancer, lung cancer, and rectal cancer, demonstrating good tolerance and minimal side effects [41, 42]. As a feed additive, VC enhances immunity and antioxidant capacity [43, 44]. In this study, we found that MT treatment led to structural damage and fatty degeneration of hepatocytes. However, the addition of 25–50 mg/kg of VC alleviated the adverse effects of MT on *C. auratus*. Notably, 150 mg/kg VC failed to mitigate MT-induced liver damage and exacerbated fatty degeneration and nuclear pyknosis. Furthermore, the addition of 50 mg/L VC to water can alleviate stress responses and liver and kidney damage in *Scophthalmus maximus* under acute cold stress [45]. In addition, VC improved the growth, feed utilization, survival rate, immunity, and antioxidant capacity of juvenile *Procambarus clarkii*. Specifically, 360.45 mg/kg VC significantly enhanced the antioxidant capacity of the hepatopancreas, whereas 487.50 mg/kg VC caused mild degenerative changes and nuclear enlargement in hepatopancreas cells [46]. This discrepancy may be due to varying species-specific requirements for dietary VC.

The inhibitory effect of MT on immune-related genes is alleviated by VC

In our study, the MT-treated group exhibited a significant increase in *TGF-β1* mRNA expression at 14 d, indicating an immunosuppressive effect. At 7 d, *TNF-α*, *IL-8*, and *TGF-β1* mRNA expression in the MT+L, MT+M, and MT+H groups exhibited varying degrees of reduction. Moreover, peripheral blood lymphocytes incubated

(A)

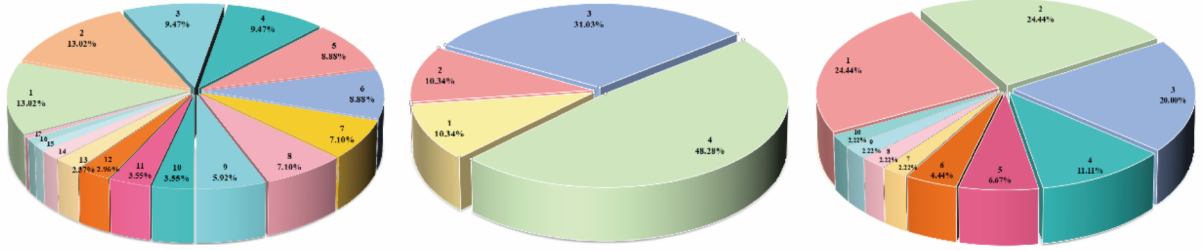

	GO term	No. unigenes
1	Cellular process	22
2	Single-organism process	22
3	Regulation of biological process	16
4	Biological regulation	16
5	Developmental process	15
6	Response to stimulus	15
7	Metabolic process	12
8	Multicellular organismal process	12
9	Signaling	10
10	Locomotion	6
11	Localization	6
12	Negative regulation of biological process	5
13	Positive regulation of biological process	4
14	Immune system process	3
15	Growth	2
16	Cellular component organization or biogenesis	2
17	Biological adhesion	1

	GO term	No. unigenes
1	Binding	14
2	Catalytic activity	9
3	Nucleic acid binding transcription factor activity	3
4	Molecular function regulator	3

	GO term	No. unigenes
1	Cell	11
2	Cell part	11
3	Organelle	9
4	Extracellular region	5
5	Extracellular matrix	3
6	Extracellular region part	2
7	Membrane	1
8	Macromolecular complex	1
9	Organelle part	1
10	Membrane part	1

(B)

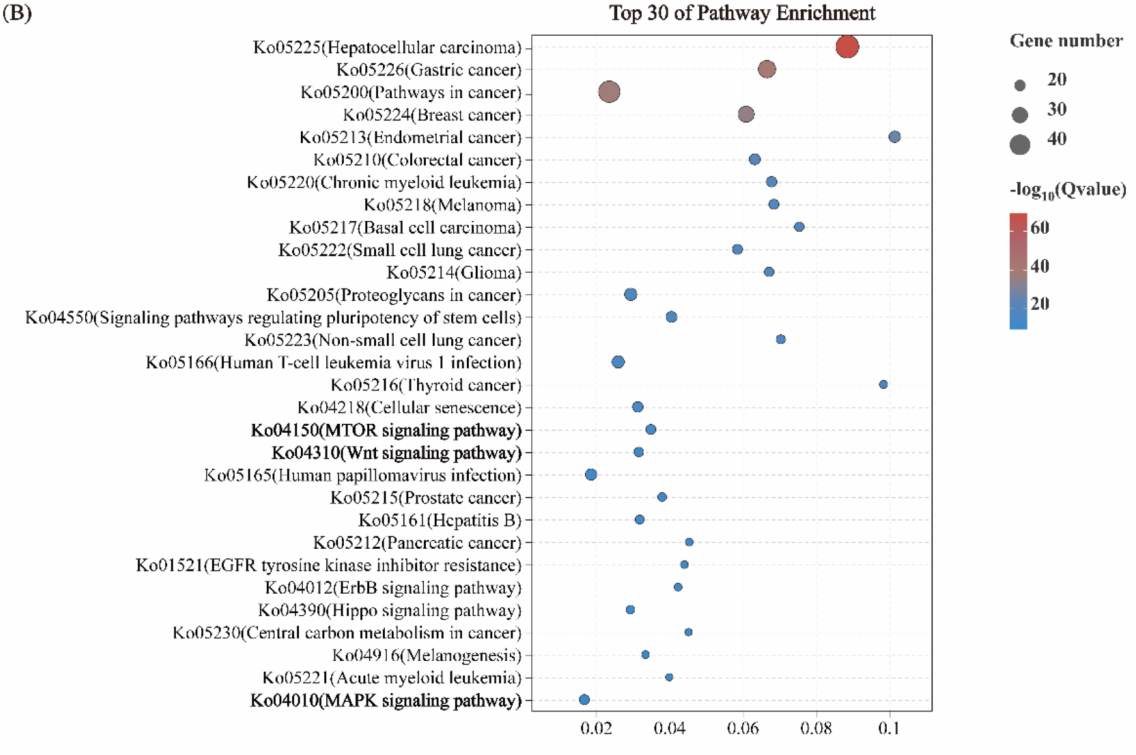

Fig. 5 Enrichment analysis results of DEGs in the hepatocellular carcinoma pathway. (A) GO enrichment pie chart showing the distribution of DEGs in the BP, CC, and MF categories. The numbers indicate the corresponding GO terms and their percentages; percentages less than 2% are not shown. (B) KEGG enrichment bubble chart showing the top 30 most enriched pathways

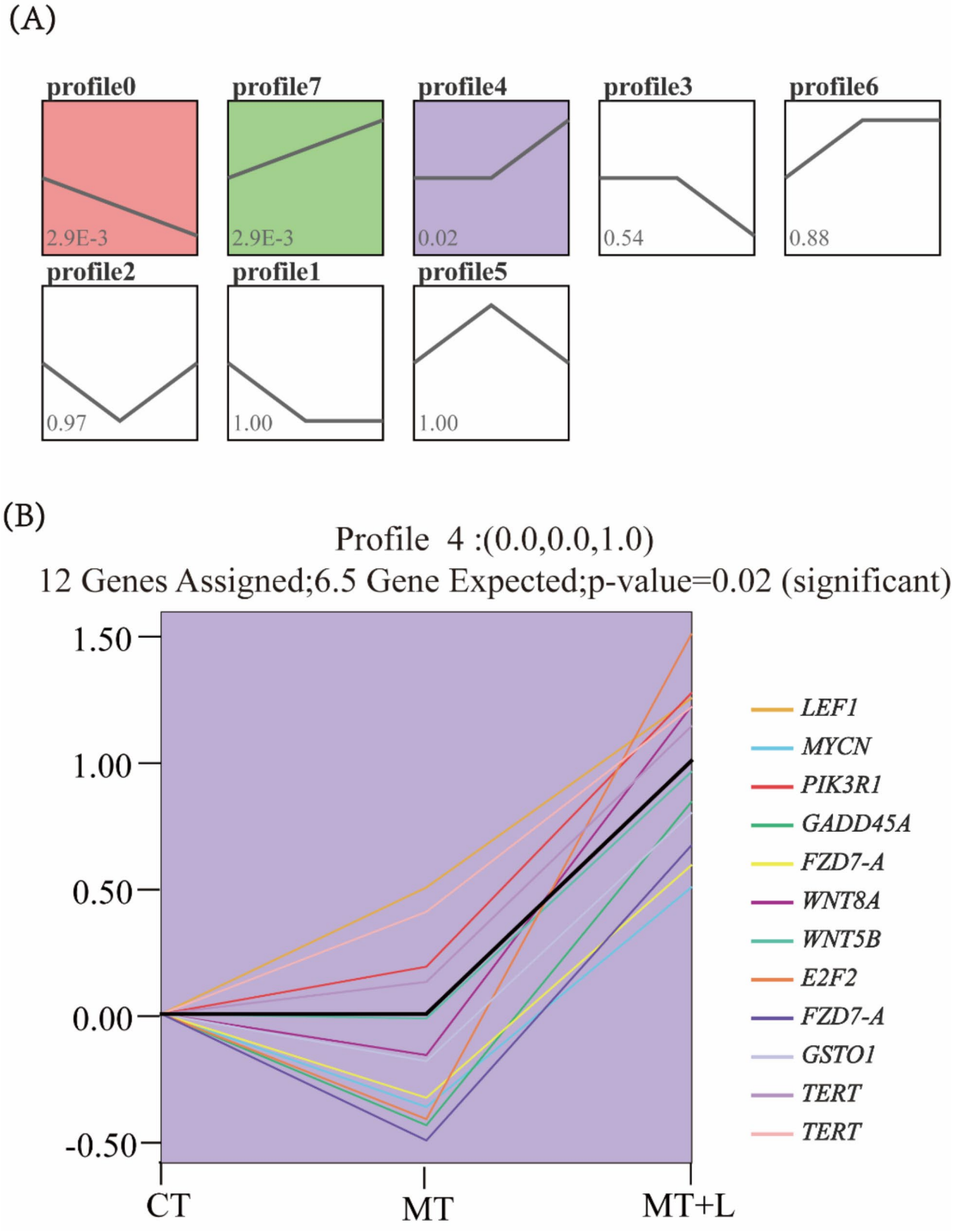

Fig. 6 Trend analysis results. (**A**) Original trend chart displaying the types, characteristics, and significance of different gene expression patterns, showing the top 20 trends. (**B**) Shading plot showing the number and expression patterns of all DEGs in different modules

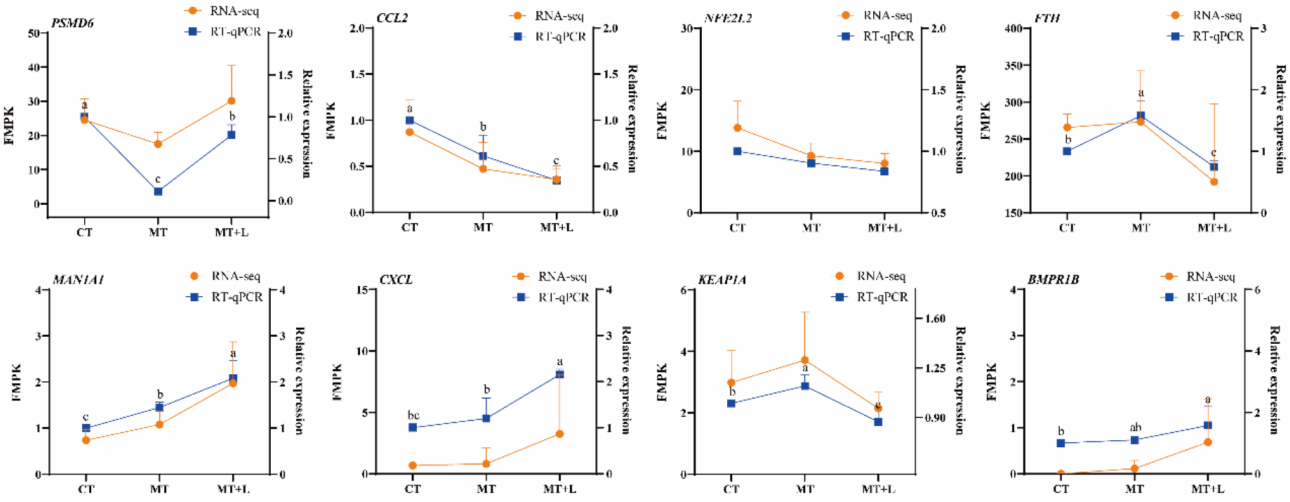

Fig. 7 Validation of DEGs. Relative mRNA expression values ($n=6$) and FPKM values ($n=3$) were calculated by comparing the treatment groups (MT and MT + L) with the control group (CT). RT-qPCR data are presented as the mean ± SD. Differences were considered statistically significant at $P<0.05$. Letters denote comparisons of RT-qPCR data

with VC can inhibit the synthesis of pro-inflammatory cytokines TNF-α and IFN-γ under lipopolysaccharide stimulation, thereby reducing inflammation [47]. However, when the exposure time was extended to 14 d, *TNF-α* and *IL-8* mRNA expression significantly increased in the MT + L and MT + M groups, whereas *TGF-β1* mRNA expression significantly increased in the MT + L and MT + H groups. This phenomenon appears contradictory to the expected anti-inflammatory effect, as TNF-α and IL-8 are typically considered pro-inflammatory cytokines, and their increase is usually associated with an exacerbation of inflammation. We speculate that the increase under the combined action of VC and MT may be a part of the cellular phagocytosis and clearance process rather than an exacerbation of inflammation [48, 49].

Chemokines, which are crucial cytokines in biological processes such as immune responses, inflammation, angiogenesis, and tumor metastasis, play key roles [50]. In our study, at 14 d, *CXC* mRNA expression significantly increased in the MT + L and MT + M groups. When the exposure time was extended to 21 d, *CXC* mRNA expression in the MT + L group remained significantly elevated. Research suggests that VC enhances the chemotaxis of neutrophils, protecting them from ROS damage and maintaining the immune barrier [51]. Therefore, we speculated that VC may affect the expression of *CXC* mRNA by enhancing the function of neutrophils, thereby regulating the inflammatory process.

Growth hormone plays various essential roles in the body, such as promoting fat breakdown, increasing protein synthesis, and regulating the sensitivity of the liver and muscles to insulin and glucose uptake [52]. Furthermore, the decrease in serum IGF-I in patients with non-alcoholic fatty liver disease is correlated with the severity of inflammation, hepatocyte ballooning [53], and fibrosis [54]. Treatment with a subcutaneous injection of IGF-I alleviated the lesions of non-alcoholic steatohepatitis [55]. In the present study, we monitored the expression of growth factors. At 7 d, *IGF-I* mRNA expression in all treatment groups significantly decreased, possibly because of the combined effects of the initial stress response, physiological adaptation, and MT. However, at 14 and 21 d, *IGF-I* mRNA expression in the MT + L, MT + M, and MT + H groups significantly increased. Additionally, VC supplementation can promote the expression of *IGF-I*, *MTOR*, and *RPS6KB1A* mRNA, thereby enhancing skeletal muscle growth in *Piaractus mesopotamicus* [56] Thus, we speculated that VC may promote the restoration and activation of the growth factor signaling pathway.

Regulation of antioxidant enzymes and related signaling pathways by VC

Oxidative stress, characterized by an elevation in intracellular ROS levels [57], triggers biological responses that can result in damage to vital biomolecules, such as DNA, proteins, and membranes [58]. VC has been shown to alleviate oxidative stress by increasing the activity of intracellular antioxidant enzymes, such as SOD, thereby significantly reducing the levels of ROS free radicals and improving the oxidative stress status [59, 60]. In our study, significantly increased GSH-PX activity was observed in the liver tissues of *C. auratus* in the MT + L, MT + M, and MT + H groups, indicating that VC enhanced the resistance of fish to oxidative stress. Treatment with 100 μg/L VC mitigated oxidative stress and behavioral disorders caused by deltamethrin and lead poisoning in *Danio rerio*, reducing lipid peroxidation

levels, regulating SOD and GSH-PX activity, and partially restoring acetylcholinesterase activity [24]. However, SOD and MDA levels were significantly elevated in the MT + H group at 14 d. While moderate supplementation of VC can enhance antioxidant enzyme activity, excessive VC may impair these systems. For instance, in *Takifugu rubripes*, SOD activity increased in a dose-dependent manner with rising VC levels but did not improve non-specific immune response when VC exceeded 160 mg/kg [61]. In *Rachycentron canadum*, high doses of VC (386.5 mg/kg) led to a decrease in lysozyme activity, a key indicator of innate immunity, without any enhancement of immune response [62]. Similar results were observed in *Ictalurus punctatus* [63] and *Salmo salar* [64]. Therefore, we speculate that the increase in SOD activity in the MT + H group may be a compensatory response to oxidative damage caused by elevated ROS levels. The significant increase in MDA levels suggests that the antioxidant system may be compromised under high VC exposure, and this oxidative imbalance could exacerbate cellular damage as high doses of VC fail to provide further protective effects.

To further investigate the impact of VC on oxidative stress and its potential mechanisms in cellular biology and health, we selected liver tissues of *C. auratus* from the CT, MT, and MT + L groups exposed for 21 d for RNA-seq analysis. We found that DEGs were significantly enriched not only in various cancer-related pathways but also in the mTOR, MAPK, and Wnt signaling pathways. In the MT treatment group, several genes associated with the mTOR pathway, such as *PTEN* and *PIK3R1*, were significantly downregulated. *PTEN*, as a tumor suppressor gene, negatively regulates the PI3K/AKT/mTOR pathway [65], whereas *PIK3R1*, a regulatory subunit of phosphoinositide 3-kinase (PI3K), plays a role in signaling for cell proliferation and survival [66]. The downregulation of these genes could lead to weakened cell growth and survival capacity, triggering apoptosis and oxidative stress. Conversely, VC reactivates the mTOR signaling pathway by upregulating genes related to cell proliferation and survival, such as *PIK3R1* and *AKT3*. This activation helps promote cell growth, proliferation, and metabolism [66, 67], countering the inhibitory effects of MT. In the MAPK pathway, MT treatment resulted in the downregulation of *PDGFA* and *IGF2*, potentially impairing cell proliferation and repair mechanisms, thereby leading to apoptosis and oxidative stress [68, 69]. In contrast, VC enhances cell proliferation and repair capacity by upregulating genes such as *IGF2* and *MK2*. Activation of the MAPK pathway enables cells to adapt to external stressors, such as oxidative stress and inflammation [70]. Studies have shown that 500 mg/kg of VC can reduce apoptosis and inflammation while enhancing autophagy through the regulation of the MAPK, PI3K/AKT/mTOR, and NF-κB signaling pathways [71]. In the Wnt signaling pathway, the upregulation of *WNT8A* in the VC treatment group suggests that VC may activate this pathway, promoting cell repair and regeneration [72]. Trend analysis revealed that MT treatment led to the downregulation of genes, such as *WNT8A*, *GADD45A*, and *GSTO1*, whereas supplementation with 25 mg/kg VC resulted in the upregulation of these genes. Upregulation of *GADD45A* expression is associated with the DNA damage response, potentially causing G2/M cell cycle arrest and apoptosis [73]. *GSTO1* is involved in antioxidant defenses, aiding in the removal of ROS and other harmful oxidative products. Thereby enhancing the antioxidant stress response capability of cells [74]. Furthermore, NRF2 is a transcription factor that can be directly or indirectly activated by ROS. Once activated, NRF2 dissociates from KEAP1, enters the nucleus, and binds to AREs to initiate the transcription of a series of antioxidant stress genes [75, 76]. In addition, VC alleviates oxidative stress via the NRF2/NQO1/HO-1 pathway [77]. Supplementing 50–100 μmol/L VC to *Ctenopharyngodon Idella* exposed to cadmium (Cd) environments can increase the expression of antioxidant responses and immune-related genes, thereby alleviating Cd-induced immune toxicity in renal cells [78]. Furthermore, a lack of VC can lead to an increase in metabolites in the purine nucleotide cycle and MDA levels in *D. rerio*, resulting in oxidative stress [79].

Conclusions

This study demonstrates that the addition of 25–50 mg/kg of VC significantly alleviates the suppressive effects of MT on the expression of liver immune-related genes in *C. auratus*, thereby reducing hepatic damage. 25 mg/kg of VC can restore the expression levels of pivotal genes such as *WNT8A*, *GADD45A*, and *GSTO1* in the liver following MT treatment. VC mitigates MT-induced inflammation, oxidative stress, and immunotoxicity by activating the mTOR, MAPK, and Wnt signaling pathways, and it may also enhance the body's antioxidant capacity through the indirect modulation of the NRF2 signaling pathway. This study provides a theoretical basis for the application of VC as a feed additive in aquaculture, suggesting its use in practical farming to improve fish health and enhance aquaculture benefits. Future research could explore the effects of VC on other aquatic organisms and its mechanisms under different environmental conditions.

Abbreviations

MT	17α-Methyltestosterone
VC	Vitamin C
EDCs	Endocrine-disrupting chemicals
HSI	Hepatic steatosis index
ROS	Reactive oxygen species
SOD	Superoxide
MDA	Malondialdehyde
GSH-PX	Glutathione peroxidase

KEAP1	NRF2/Kelch-like ECH-associated protein 1
ARE	Antioxidant response elements
DEGs	Differentially expressed genes
GO	Gene ontology
KEGG	Kyoto encyclopedia of genes and genomes
MF	Molecular Functions
BP	Biological Processes
CC	Cellular Components
TNF-α	Tumor necrosis factor-alpha
IL-8/10	Interleukin-8/10
IFN-γ	Interferon-gamma
TGF-β1	Transforming growth factor-beta 1
CXC	Chemokine (C-X-C motif)
Caspase-9	Cysteinyl aspartate specific proteinase 9
IGF-I	Insulin-like growth factor I
PSMD6	proteasome non-ATPase regulatory subunit 6
CCL2	C-C motif chemokine 2
CXCL	C-X-C motif chemokine 2
NFE2L2	Nuclear factor erythroid 2-related factor 2
FTH	Ferritin
MAN1A1	Mannosyl-oligosaccharide 1
BMPR1B	Bone morphogenetic protein receptor type-1B

Acknowledgements
We would like to thank Elsevier (www.elsevier.cn) for English language editing.

Author contributions
TYL, ZJX, and HYZ conceived, designed, and coordinated this research. YL, WYR, YC, GC, and LC performed the data analyses and wrote the initial version of the manuscript. QL, JS, WWW, YL, XZW, and SZL collected samples. All authors interpreted the results and edited the manuscript. All authors read and approved the final manuscript.

Funding
This study was supported by grants from the Natural science foundation of Shanxi Province (202103021224136), the National Natural Science Foundation of China (31600416), "1331 Project" Key Disciplines of Animal Sciences, Shanxi Province (J201911306), Fishery Industrial Technology System of Shanxi Province (65721G0203010), Shanxi Key Laboratory of Animal Genetics Resource Utilization and Breeding, the Youth Project of the National Natural Science Foundation of China (NNSFC) (32302997), and the Youth Project of Natural Science Foundation of Shandong Province (ZR2023QC113).

Data availability
The raw sequencing reads from the RNA-seq described in this study have been deposited in the NCBI Sequence Read Archive under accession number [PRJNA1141099] (https://www.ncbi.nlm.nih.gov/bioproject/PRJNA1141099). Additional data supporting the findings of this study are provided within the manuscript and in the supplementary information files.

Declarations

Ethics approval and consent to participate
This study was approved by the Animal Protection and Ethics Committee of Shanxi Agricultural University, approval number IACUC No. SXAU-EAW-2018G.R.0201. Throughout the experiment, all fish were anesthetized with MS-222 (1: 10,000) to minimize suffering as much as possible.

Consent for publication
Not applicable.

Competing interests
The authors declare no competing interests.

Euthanasia and anesthesia methods
MS-222 is a widely used anesthetic for aquatic animals, particularly in experimental research and euthanasia procedures that prioritize animal welfare. MS-222 effectively alleviates pain and stress in fish during experimental processes. When using MS-222 for anesthesia, it is first diluted to the recommended concentration (typically 25–30 g/m^3) and then added to water that has been aerated for 24 h. The fish are immersed in this solution for 15–20 min, with observation until the desired anesthetic effect is achieved.

Received: 24 July 2024 / Accepted: 28 October 2024
Published online: 11 November 2024

References

1. Cano R, Pérez JL, Dávila LA, Ortega Á, Gómez Y, Valero-Cedeño NJ, Parra H, Manzano A, Véliz Castro TI, Albornoz MPD, Cano G, Rojas-Quintero J, Chacín M, Bermúdez V. Role of endocrine-disrupting chemicals in the pathogenesis of non-alcoholic fatty liver disease: a comprehensive review. Int J Mol Sci. 2021;22(9):4807. https://doi.org/10.3390/ijms22094807.
2. Liu S, Chen Y, Li T, Qiao L, Yang Q, Rong W, Liu Q, Wang W, Song J, Wang X, Liu Y. Effects of 17α-methyltestosterone on the transcriptome and sex hormones in the brain of *Gobiocypris rarus*. Int J Mol Sci. 2023;24(4):3571. https://doi.org/10.3390/ijms24043571. .
3. Rong W, Chen Y, Xiong Z, Zhao H, Li T, Liu Q, Song J, Wang X, Liu Y, Liu S. Effects of combined exposure to polystyrene microplastics and 17α-Methyltestosterone on the reproductive system of zebrafish. Theriogenology. 2024;215:158–69. https://doi.org/10.1016/j.theriogenology.2023.12.004. .
4. Saaristo M, Wong BB, Mincarelli L, Craig A, Johnstone CP, Allinson M, Lindstrom K, Craft JA. Characterisation of the transcriptome of male and female wild-type guppy brains with RNA-Seq and consequences of exposure to the pharmaceutical pollutant, 17α-ethinyl estradiol. Aquat Toxicol. 2017;186:28–39. https://doi.org/10.1016/j.aquatox.2017.02.016.
5. Carter G, Ward J. Independent and synergistic effects of microplastics and endocrine-disrupting chemicals on the reproductive social behavior of fathead minnows (*Pimephales promelas*). Ecol Evol. 2024;14(2):e10846. https://doi.org/10.1002/ece3.10846.
6. Kwon W, Kim D, Kim HY, Jeong SW, Lee SG, Kim HC, Lee YJ, Kwon MK, Hwang JS, Han JE, Park JK, Lee SJ, Choi SK. Microglial phagocytosis of polystyrene microplastics results in immune alteration and apoptosis in vitro and *in vivo*. Sci Total Environ. 2022;807(2):150817. https://doi.org/10.1016/j.scitotenv.2021.150817.
7. Chen W, Lau SW, Fan Y, Wu RSS, Ge W. Juvenile exposure to bisphenol A promotes ovarian differentiation but suppresses its growth-potential involvement of pituitary follicle stimulating hormone. Aquat Toxicol. 2017;193:111–21. https://doi.org/10.1016/j.aquatox.2017.10.008. .
8. Liu S, Yang Q, Zhou J, Cao X, Chen Y, Liu Q, Wang W, Song J. Effects of 17α-methyltestosterone on lipid metabolism in liver of *Gobiocypris rarus*. Asian J Ecotoxicol. 2021;16(5):87–101. https://doi.org/10.7524/AJE.1673-5897.20210602002. .
9. Syeda MZ, Hong T, Huang C, Huang W, Mu Q. B cell memory: from generation to reactivation: a multipronged defense wall against pathogens. Cell Death Discov. 2024;10(1):117. https://doi.org/10.1038/s41420-024-01889-5.
10. Trigunaite A, Dimo J, Jorgensen TN. Suppressive effects of androgens on the immune system. Cell Immunol. 2015;294:87–94. https://doi.org/10.1016/j.cellimm.2015.02.004. .
11. Zheng X, Wu Y, Bi J, Huang Y, Cheng Y, Li Y, Wu Y, Cao G, Tian Z. The use of supercytokines, immunocytokines, engager cytokines, and other synthetic cytokines in immunotherapy. Cell Mol Immunol. 2022;19(2):192–209. https://doi.org/10.1038/s41423-021-00786-6.
12. Liu F, Yang Y, Fan XW, Zhang N, Wang S, Shi YJ, Hu WJ, Wang CX. Impacts of inflammatory cytokines on depression: a cohort study. BMC Psychiatry. 2024;24(1):195. https://doi.org/10.1186/s12888-024-05639-w. .
13. Leet JK, Richter CA, Claunch RA, Gale RW, Tillitt DE, Iwanowicz LR. Immunomodulation in adult largemouth bass (*Micropterus salmoides*) exposed to a model estrogen or mixture of endocrine disrupting contaminants during early gonadal recrudescence. Comp Immunol Rep. 2024;6:200140. https://doi.org/10.1016/j.cirep.2024.200140. .
14. Backe WJ, Ort C, Brewer AJ, Field JA. Analysis of androgenic steroids in environmental waters by large-volume injection liquid chromatography tandem mass spectrometry. Anal Chem. 2011;83(7):2622–30. https://doi.org/10.1021/ac103013h.
15. Xie Y, Gao Z, Ren Y. Trace analysis of five androgens in environmental waters by optimization of enzymolysis and solid-phase extraction ultra-performance liquid chromatography-mass spectrometry and its risk assessment. Environ Toxicol Chem. 2024;43(4):915–25. https://doi.org/10.1002/etc.5805.

16. Hornung MW, Jensen KM, Korte JJ, Kahl MD, Durhan EJ, Denny JS, Henry TR, Ankley GT. Mechanistic basis for estrogenic effects in fathead minnow (*Pimephales promelas*) following exposure to the androgen 17alpha-methyltestosterone: conversion of 17alpha-methyltestosterone to 17alpha-methylestradiol. Aquat Toxicol. 2004;66(1):15–23. https://doi.org/10.1016/j.aquatox.2003.06.004. .
17. Phumyu N, Boonanuntanasarn S, Jangprai A, Yoshizaki G, Na-Nakorn U. Pubertal effects of 17α-methyltestosterone on GH-IGF-related genes of the hypothalamic-pituitary-liver-gonadal axis and other biological parameters in male., female and sex-reversed Nile tilapia. Gen Comp Endocrinol. 2012;177(2):278–92. https://doi.org/10.1016/j.ygcen.2012.03.008.
18. Liu S, Xu P, Liu X, Guo D, Chen X, Bi S, Lai H, Wang G, Zhao X, Su Y, Yi H, Zhang Y, Li G. Production of neo-male mandarin fish *Siniperca chuatsi* by masculinization with orally administered 17α-methyltestosterone. Aquaculture. 2021;530:735904. https://doi.org/10.1016/j.aquaculture.2020.735904. .
19. Abo-Al-Ela HG, El-Nahas AF, Mahmoud S, Ibrahim EM. The extent to which immunity, apoptosis and detoxification gene expression interact with 17 alpha-methyltestosterone. Fish Shellfish Immunol. 2017;60:289–98. https://doi.org/10.1016/j.fsi.2016.11.057.
20. Hild SA, Attardi BJ, Koduri S, Till BA, Reel JR. Effects of synthetic androgens on liver function using the rabbit as a model. J Androl. 2010;31(5):472–81. https://doi.org/10.2164/jandrol.109.009365.
21. Cuesta A, Vargas-Chacoff L, García-López A, Arjona FJ, Martínez-Rodríguez G, Meseguer J, Mancera JM, Esteban MA. Effect of sex-steroid hormones, testosterone and estradiol, on humoral immune parameters of gilthead seabream. Fish Shellfish Immunol. 2007;23(3):693–700. https://doi.org/10.1016/j.fsi.2007.01.015.
22. Abo-Al-Ela HG, El-Nahas AF, Mahmoud S, Ibrahim EM. Vitamin C modulates the immunotoxic effect of 17α-methyltestosterone in Nile tilapia. Biochemistry. 2017;56(14):2042–50. https://doi.org/10.1021/acs.biochem.6b01284.
23. Yin X, Chen K, Cheng H, Chen X, Feng S, Song Y, Liang L. Chemical stability of ascorbic acid integrated into commercial products: a review on bioactivity and delivery technology. Antioxid (Basel). 2022;11(1):153. https://doi.org/10.3390/antiox11010153. .
24. Paduraru E, Flocea EI, Lazado CC, Simionov IA, Nicoara M, Ciobica A, Faggio C, Jijie R. Vitamin C mitigates oxidative stress and behavioral impairments induced by deltamethrin and lead toxicity in zebrafish. Int J Mol Sci. 2021;22(23):12714. https://doi.org/10.3390/ijms222312714. .
25. Poli V, Madduru R, Aparna Y, Kandukuri V, Motireddy SR. Amelioration of cadmium-induced oxidative damage in Wistar rats by vitamin C, zinc and N-acetylcysteine. Med Sci (Basel). 2022;10(1):7–14. https://doi.org/10.3390/medsci10010007. .
26. Ferronato G, Tavakoli M, Bouyeh M, Seidavi A, Suárez Ramírez L, Prandini A. Effects of combinations of dietary vitamin C and acetylsalicylic acid on growth performance, carcass traits and, serum and immune response parameters in broilers. Anim (Basel). 2024;14(4):649. https://doi.org/10.3390/ani14040649. .
27. Sun J, Li X, Lu K, Waang L, Song K, Zhang C. Effects of dietary vitamin C on the immune., antioxidant capacity and stress tolerance of spotted seabass (*Lateolabrax Maculatus*) after acute cooling. Progress Fish Sci. 2021;42(4):126–33. https://doi.org/10.1016/j.fsi.2012.01.024.
28. Grüning NM, Ralser M. Monogenic disorders of ROS production and the primary anti-oxidative defense. Biomolecules. 2024;14(2):206. https://doi.org/10.3390/biom14020206.
29. Erdogan Z, Erdogan S, Celik S, Unlu A. Effects of ascorbic acid on cadmium-induced oxidative stress and performance of broilers. Biol Trace Elem Res. 2005;104(1):19–32. https://doi.org/10.1385/BTER:104:1:019.
30. Moretti M, Budni J, Dos Santos DB, Antunes A, Daufenbach JF, Manosso LM, Farina M, Rodrigues AL. Protective effects of ascorbic acid on behavior and oxidative status of restraint-stressed mice. J Mol Neurosci. 2013;49(1):68–79. https://doi.org/10.1007/s12031-012-9892-4. .
31. Wu L, Xu W, Li H, Dong B, Geng H, Jin J, Han D, Liu H, Zhu X, Yang Y, Xie S. Vitamin C attenuates oxidative stress, inflammation, and apoptosis induced by acute hypoxia through the nrf2/keap1 signaling pathway in gibel carp (*Carassius gibelio*). Antioxid (Basel). 2022;11(5):935. https://doi.org/10.3390/antiox11050935.
32. Pant T, Uche N, Juric M, Zielonka J, Bai X. Regulation of immunomodulatory networks by Nrf2-activation in immune cells: Redox control and therapeutic potential in inflammatory diseases. Redox Biol. 2024;70:103077. https://doi.org/10.1016/j.redox.2024.103077. .
33. Zhou J, Zheng Q, Chen Z. The NRF2 pathway in liver diseases. Front Cell Dev Biol. 2022;10:826204. https://doi.org/10.3389/fcell.2022.826204. .
34. Chen H, Jin S, Guo J, Kombairaju P, Biswal S, Zirkin BR. Knockout of the transcription factor Nrf2: effects on testosterone production by aging mouse leydig cells. Mol Cell Endocrinol. 2015;409:113–20. https://doi.org/10.1016/j.mce.2015.03.013. .
35. Xu H, Jiang W, Feng L, Liu Y, Wu P, Jiang J, Kuang S, Tang L, Tang W, Zhang Y, Zhou X. Dietary vitamin C deficiency depresses the growth, head kidney and spleen immunity and structural integrity by regulating NF-κB, TOR, Nrf2, apoptosis and MLCK signaling in young grass carp (*Ctenopharyngodon idella*). Fish Shellfish Immunol. 2016;52:111–38. https://doi.org/10.1016/j.fsi.2016.02.033. .
36. Mi S, Yin X, Li J, Zhang Z, Wu P, Xian J, Wang D. The Influence of Vitamin C on the non-specific immunity of *Procambarus clarkii*. Hebei Fisheries. 2022;2:7–10. https://doi.org/10.3969/j.issn.1004-6755.2022.02.002. (in Chinese).
37. Yue Z, Li X, Zhao Y, Xiang J, Liu Y. Study on miniaturization of determination of vitamin C by direct iodometry in laboratory. J Shanxi Datong Univ (Natural Sci Edition). 2022;38(2):8–1044. https://doi.org/10.3969/j.issn.1674-0874.2022.02.003. (in Chinese).
38. Wang J, Zhou J, Yang Q, Wang W, Liu Q, Liu W, Liu S. Effects of 17 α-methyltestosterone on the transcriptome, gonadal histology and sex steroid hormones in *Pseudorasbora parva*. Theriogenology. 2020;155:88–97. https://doi.org/10.1016/j.theriogenology.2020.05.035. .
39. Chen Z, Omori Y, Koren S, Shirokiya T, Kuroda T, Miyamoto A. De novo assembly of the goldfish (*Carassius auratus*) genome and the evolution of genes after whole-genome duplication. Sci Adv. 2019;5:eaav0547. https://doi.org/10.1126/sciadv.aav05479.
40. Hild SA, Attardi BJ, Koduri S, Till BA, Reel JR. Effects of synthetic androgens on liver function using the rabbit as a mode. J Androl. 2010;31(5):472–81. https://doi.org/10.2164/jandrol.109.009365. .
41. Yin L, Qi S, Zhu Z. Advances in mitochondria-centered mechanism behind the roles of androgens and androgen receptor in the regulation of glucose and lipid metabolism. Front Endocrinol (Lausanne). 2023;14:1267170. https://doi.org/10.3389/fendo.2023.1267170. .
42. Doseděl M, Jirkovský E, Macáková K, Krčmová LK, Javorská L, Pourová J, Mercolini L, Remião F, Nováková L, Mladěnka P. On Behalf of the Oemonom. Vitamin C-sources, physiological role, kinetics, deficiency, use, toxicity, and determination. Nutrients. 2021;13(2):615. https://doi.org/10.3390/nu13020615.
43. Otanwa OO, Ndidi US, Ibrahim AB, Balogun EO, Anigo KM. Prooxidant effects of high dose ascorbic acid administration on biochemical., haematological and histological changes in *Cavia porcellus* (Guinea pigs): a Guinea pig experimental model. Pan Afr Med J. 2023;46:18. https://doi.org/10.11604/pamj.2023.46.18.36098. .
44. Gęgotek A, Skrzydlewska E. Antioxidative and anti-inflammatory activity of ascorbic acid. Antioxid (Basel). 2022;11(10):1993. https://doi.org/10.3390/antiox11101993. .
45. Hieu TV, Guntoro B, Qui NH, Quyen NTK, Hafiz FAA. The application of ascorbic acid as a therapeutic feed additive to boost immunity and antioxidant activity of poultry in heat stress environment. Vet World. 2022;15(3):685–93. https://doi.org/10.14202/vetworld.2022.685-693. .
46. Jing L, Hua M, Zhang C, Huang B, Tang J, Zhang J. Effects of vitamin C pretreatment on physiology, biochemistry, and meat quality of Scophthalmus maximus under cold stress. Fujian J Agricultural Sci. 2022;37(10):1256–65. https://doi.org/10.19303/j.issn.1008-0384.2022.010.003.
47. Molina N, Morandi AC, Bolin AP, Otton R. Comparative effect of fucoxanthin and vitamin C on oxidative and functional parameters of human lymphocytes. Int Immunopharmacol. 2014;22(1):41–50. https://doi.org/10.1016/j.intimp.2014.06.026.
48. Härtel C, Strunk T, Bucsky P, Schultz C. Effects of vitamin C on intracytoplasmic cytokine production in human whole blood monocytes and lymphocytes. Cytokine. 2004;27(4–5):101–6. https://doi.org/10.1016/j.cyto.2004.02.004.
49. Prabudi MO, Siregar MFG, Nasution IPA, Ilyas S. The effect of ascorbic acid on interleukin-10 and tumor necrosis factor-α cytokines in rattus norvegicus with endometritis. Open Access Maced J Med Sci. 2021;9:798–801. https://doi.org/10.3889/oamjms.2021.6946.
50. Ren H, Yang X, Hou W, Meng J, Luo D, Zhang C. Comprehensive analysis of the clinical and biological significances for chemokine CXCL3 in cholangiocarcinoma. Med (Baltim). 2024;103(11):e37460. https://doi.org/10.1097/MD.0000000000037460.
51. Elste V, Troesch B, Eggersdorfer M, Weber P. Emerging evidence on neutrophil motility supporting its usefulness to define vitamin C intake requirements. Nutrients. 2017;9(5):503. https://doi.org/10.3390/nu9050503.

52. Takahashi Y. The role of growth hormone and insulin-like growth factor-1 in the liver. Int J Mol Sci. 2017;18(7):1447. https://doi.org/10.3390/ijms18071447.
53. Dichtel LE, Corey KE, Misdraji J, Bredella MA, Schorr M, Osganian SA, Young BJ, Sung JC, Miller KK. The association between IGF-1 levels and the histologic severity of nonalcoholic fatty liver disease. Clin Transl Gastroenterol. 2017;8(1):e217. https://doi.org/10.1038/ctg.2016.72. .
54. Sumida Y, Yonei Y, Tanaka S, Mori K, Kanemasa K, Imai S, Taketani H, Hara T, Seko Y, Ishiba H, Okajima A, Yamaguchi K, Moriguchi M, Mitsuyoshi H, Yasui K, Minami M, Itoh Y. Lower levels of insulin-like growth factor-1 standard deviation score are associated with histological severity of non-alcoholic fatty liver disease. Hepatol Res. 2015;45(7):771–81. https://doi.org/10.1111/hepr.12408.
55. Nishizawa H, Takahashi M, Fukuoka H, Iguchi G, Kitazawa R, Takahashi Y. GH-independent IGF-I action is essential to prevent the development of non-alcoholic steatohepatitis in a GH-deficient rat model. Biochem Biophys Res Commun. 2012;423(2):295–300. https://doi.org/10.1016/j.bbrc.2012.05.115.
56. Zanella BTT, Magiore IC, Duran BOS, Pereira GG, Vicente IST, Carvalho PLPF, Salomão RAS, Mareco EA, Carvalho RF, Paula TG, Barros MM, Dal-Pai-Silva M. Ascorbic acid supplementation improves skeletal muscle growth in pacu (*Piaractus mesopotamicus*) juveniles: in vivo and in vitro studies. Int J Mol Sci. 2021;22(6):2995. https://doi.org/10.3390/ijms22062995. .
57. Jomova K, Raptova R, Alomar SY, Alwasel SH, Nepovimova E, Kuca K, Valko M. Reactive oxygen species, toxicity, oxidative stress, and antioxidants: chronic diseases and aging. Arch Toxicol. 2023;97(10):2499–574. https://doi.org/10.1007/s00204-023-03562-9.
58. Liguori I, Russo G, Curcio F, Bulli G, Aran L, Della-Morte D, Gargiulo G, Testa G, Cacciatore F, Bonaduce D, Abete P. Oxidative stress, aging, and diseases. Clin Interv Aging. 2018;13:757–72. https://doi.org/10.2147/CIA.S158513. .
59. Zhou QC, Wang L, Wang H, Xie F, Wang T. Effect of dietary vitamin C on the growth performance and innate immunity of juvenile cobia (*Rachycentron canadum*). Fish Shellfish Immunol. 2012;32(6):969–75. https://doi.org/10.1016/j.fsi.2012.01.024.
60. El-Garawani IM, Khallaf EA, Alne-Na-Ei AA, Elgendy RG, Mersal GAM, El-Seedi HR. The role of ascorbic acid combined exposure on Imidacloprid-induced oxidative stress and genotoxicity in Nile tilapia. Sci Rep. 2021;11(1):14716. https://doi.org/10.1038/s41598-021-94020-y. .
61. Eo J, Lee KJ. Effect of dietary ascorbic acid on growth and non-specific immune responses of tiger puffer, *Takifugu rubripes*. Fish Shellfish Immunol. 2008;25(5):611–6. https://doi.org/10.1016/j.fsi.2008.08.009.
62. Zhou Q, Wang L, Wang H, Xie F, Wang T. Effect of dietary vitamin C on the growth performance and innate immunity of juvenile cobia (*Rachycentron canadum*). Fish Shellfish Immunol. 2012;32(6):969–75. https://doi.org/10.1016/j.fsi.2012.01.024.
63. Li MH, Johnson MR, Robinson EH. Elevated dietary vitamin C concentrations did not improve resistance of channel catfish, *Ictalurus punctatus*, against *Edwardsiella ictaluri* infection. Aquaculture. 1993;117:303–12. https://api.semanticscholar.org/CorpusID:83709168.
64. Thompson I, White A, Fletcher TC, Houlihan DF, Secombes CJ. The effect of stress on the immune response of Atlantic salmon (*Salmo salar L.*) fed diets containing different amounts of vitamin C. Aquaculture. 1993;114:1–18. https://doi.org/10.1016/0044-8486(93)90246-U.
65. Haddadi N, Lin Y, Travis G, Simpson AM, Nassif NT, McGowan EM. PTEN/PTENP1: regulating the regulator of RTK-dependent PI3K/Akt signalling, new targets for cancer therapy. Mol Cancer. 2018;17(1):37. https://doi.org/10.1186/s12943-018-0803-3.
66. Fruman DA, Rommel C. PI3K and cancer: lessons, challenges and opportunities. Nat Rev Drug Discov. 2014;13(2):140–56. https://doi.org/10.1038/nrd4204.
67. Jin Y, Sui HJ, Dong Y, Ding Q, Qu WH, Yu SX, Jin YX. Atorvastatin enhances neurite outgrowth in cortical neurons in vitro via up-regulating the Akt/mTOR and Akt/GSK-3β signaling pathways. Acta Pharmacol Sin. 2012;33(7):861–72. https://doi.org/10.1038/aps.2012.59.
68. LeRoith D, Holly JMP, Forbes BE. Insulin-like growth factors: ligands, binding proteins, and receptors. Mol Metab. 2021;52:101245. https://doi.org/10.1016/j.molmet.2021.101245.
69. Contreras O, Córdova-Casanova A, Brandan E. PDGF-PDGFR network differentially regulates the fate, migration, proliferation, and cell cycle progression of myogenic cells. Cell Signal. 2021;84:110036. https://doi.org/10.1016/j.cellsig.2021.110036.
70. Rezatabar S, Karimian A, Rameshknia V, Parsian H, Majidinia M, Kopi TA, Bishayee A, Sadeghinia A, Yousefi M, Monirialamdari M, Yousefi B. RAS/MAPK signaling functions in oxidative stress, DNA damage response and cancer progression. J Cell Physiol. 2019;234(9):14951–65. https://doi.org/10.1002/jcp.28334.
71. Cui YN, Tian N, Luo YH, Zhao JJ, Bi CF, Gou Y, Liu J, Feng K, Zhang JF. High-dose vitamin C injection ameliorates against sepsis-induced myocardial injury by anti-apoptosis, anti-inflammatory and pro-autophagy through regulating MAPK, NF-κB and PI3K/AKT/mTOR signaling pathways in rats. Aging. 2024;16(8):6937–53. https://doi.org/10.18632/aging.205735.
72. Xu X, Zhang M, Xu F, Jiang S. Wnt signaling in breast cancer: biological mechanisms, challenges and opportunities. Mol Cancer. 2020;19(1):165. https://doi.org/10.1186/s12943-020-01276-5.
73. Yang F, Liu WW, Chen H, Zhu J, Huang AH, Zhou F, Gan Y, Zhang YH, Ma L. Carfilzomib inhibits the growth of lung adenocarcinoma via upregulation of Gadd45a expression. J Zhejiang Univ Sci B. 2020;21(1):64–76. https://doi.org/10.1631/jzus.B1900551.
74. Lee JM, Lee JH, Song MK, Kim YJ. NXP032 ameliorates aging-induced oxidative stress and cognitive impairment in mice through activation of Nrf2 signaling. Antioxid (Basel). 2022;11(1):130. https://doi.org/10.3390/antiox11010130.
75. Deshmukh P, Unni S, Krishnappa G, Padmanabhan B. The Keap1-Nrf2 pathway: promising therapeutic target to counteract ROS-mediated damage in cancers and neurodegenerative diseases. Biophys Rev. 2017;9(1):41–56. https://doi.org/10.1007/s12551-016-0244-4.
76. He F, Ru X, Wen T. NRF2, a transcription factor for stress response and beyond. Int J Mol Sci. 2020;21(13):4777. https://doi.org/10.3390/ijms21134777. .
77. Xu LL, Zhao B, Sun SL, Yu SF, Wang YM, Ji R, Yang ZT, Ma L, Yao Y, Chen Y, Sheng HQ, Chen EZ, Mao EQ. High-dose vitamin C alleviates pancreatic injury via the NRF2/NQO1/HO-1 pathway in a rat model of severe acute pancreatitis. Ann Transl Med. 2020;8(14):852. https://doi.org/10.21037/atm-19-4552.
78. Yin Y, Zhang P, Liu J, Wang N, Shang X, Zhang Y, Li Y. Amelioration of cd-induced oxidative stress, mt gene expression, and immune damage by vitamin C in grass carp kidney cells. Biol Trace Elem Res. 2020;194(2):552–9. https://doi.org/10.1007/s12011-019-01808-1.
79. Kirkwood JS, Lebold KM, Miranda CL, Wright CL, Miller GW, Tanguay RL, Barton CL, Traber MG, Stevens JF. Vitamin C deficiency activates the purine nucleotide cycle in zebrafish. J Biol Chem. 2012;287(6):3833–41. https://doi.org/10.1074/jbc.M111.316018. .

Publisher's note